Irreversible crumpling of graphene from hydrostatic and biaxial compression

IOP Publishing Journal of Physics D: Applied Physics
J. Phys. D: Appl. Phys. **51** (2018) 015302 (8pp) https://doi.org/10.1088/1361-6463/aa99af

Irreversible crumpling of graphene from hydrostatic and biaxial compression

Jing Wan[1], Jin-Wu Jiang[1] and Harold S Park[2]

[1] Shanghai Institute of Applied Mathematics and Mechanics, Shanghai Key Laboratory of Mechanics in Energy Engineering, Shanghai University, Shanghai 200072, People's Republic of China
[2] Department of Mechanical Engineering, Boston University, Boston, MA 02215, United States of America

E-mail: jwjiang5918@hotmail.com

Received 9 September 2017, revised 8 November 2017
Accepted for publication 10 November 2017
Published 4 December 2017

Abstract

We perform molecular dynamics simulations to investigate the irreversibility of crumpled graphene obtained by hydrostatic or biaxial compression. Our results show that there is a critical degree of crumpling, above which the crumpling is irreversible after the external force is removed. The critical degree of irreversible crumpling is closely related to the self-adhesion phenomenon of graphene, which leads to a step-like jump or decrease in the adhesion energy. We find the critical degree of crumpling is about 0.5 or 0.55 for hydrostatic or biaxial compression, which matches analytic predictions based on a competition between adhesive and bending energies in folded graphene.

Keywords: crumpled graphene, irreversibility, degree of crumpling

(Some figures may appear in colour only in the online journal)

1. Introduction

Crumpling is a general physical phenomenon that exists in thin sheets and membranes [1–3]. Previous studies have shown that monolayer graphene [4] can be easily bent, resulting in ripples, folds or crumples [5–7]. It has been shown that geometry has important effects on the physical properties and the performance of carbon nanostructures [8–10]. In particular, much interest has been attracted by three-dimensional (3D) graphene nanostructures, [10, 11] for which crumpled graphene is one of the main building blocks. It was found that crumpled graphene-based materials are promising candidates for applications in supercapacitors, [11–13] electronics, [14] gas storage, [15] separation [16] and electrode materials, [17] amongst others.

There are many high-density deformations (ripples, folds and wrinkles) in crumpled graphene, [10, 11, 18] which strongly affects the mechanical properties of graphene [8, 9, 14, 19–21]. Unlike flat graphene, crumpled graphene shows a non-linear stress-strain response even in the small strain range [22]. Furthermore, experimental results show that crumpled graphene nanosheets can be used as a highly effective gas barrier, for example by inhibiting the permeation of oxygen molecules [23]. Supercapacitor cells constructed with crumpled graphene yield high values of gravimetric capacitance and energy density, and the processes used to make the crumpled graphene are readily scalable to industrial levels. Han *et al* [24] found outstanding compressibility of holey graphene, which not only enables the fabrication of robust, dense graphene graphene products thats exhibit high density (1.4 g cm^{-3}), excellent specific mechanical strength [18 MPa (g/cm^3)], and good electrical (130 S cm^{-1}) and thermal (20 W mK^{-1}) conductivities, but also provides a binder-free dry process that overcomes the disadvantages of wet processes required for fabrication of three-dimensional graphene products [25].

Crumpled graphene has both high free pore volume and high compressive strength, and shows no significant reduction in the accessible surface area even under compact compression, [9] where the specific structure of crumpled graphene can be well described by the degree of crumpling. It was found that the degree of crumpling has strong effects on the performance of graphene-based devices [8, 9, 14]. However, an interesting issue that has not been resolved are the factors and mechanisms governing whether the crumpling of graphene is reversible or irreversible, where irreversibility implies that

crumpled graphene is unable to recover its initially flat configuration after the removal of external constraints.

In this paper, we perform molecular dynamics (MD) simulations to study the behavior of crumpled graphene obtained from hydrostatic or biaxial compression. Our focus is on the factors governing irreversible crumpling of graphene. In doing so, we demonstrate a critical degree of crumpling, above which the crumpled graphene becomes irreversible after the removal of the external constraints. This is related to the self-adhesion of graphene, which results in a sudden decrease in the adhesion energy due to an increase in van der Waals (vdW) interactions. This critical degree of crumpling is found to be about 0.5 or 0.55 for hydrostatic or biaxial compression, respectively. These results match analytic predictions based on the competition between adhesive and bending energies in folded graphene.

2. Structure and simulation details

Figure 1 illustrates two resultant crumpled graphene sheets which had dimensions of 20 × 20 nm in the initially flat configuration. The structures in figures 1(a) and (b) are obtained by hydrostatic compression and biaxial compression, respectively. The structures we consider in the present work are pristine, without any defects or contamination that may arise from an experimental fabrication and transfer process. It is possible that if graphene is highly defective that it can be crumpled by thermal perturbations and fluctuations. However, most synthesis processes do involve an annealing-like step to reduce any residual contamination. The two crumpling processes are simulated by following the procedures illustrated in figures 1(c) and (d). For the hydrostatic compression, which has been performed in other papers, [13, 22, 26, 27] graphene is crumpled by shrinking a spherical shell with an initial radius R_0, a constant stiffness $k = 8.0$ GPa and a constant shrinking rate $\tau = 10$ m/s. Specifically, the analytical force $f(r) = k(r - R)^2$ is applied to each atom in the system during the shrinking process, where r is the radial distance of each atom from the center of the spherical shell. We note that we also investigated two other force forms, $f(r) = kr^2$ and $f(r) = k(r - R)$, and similar results were obtained. Hence the form of this analytical force does not affect the hydrostatic compression process. The value of k is chosen so that the crumpled graphene is able to achieve a compact structure that is close to a completely collapsed state. The shrinking rate τ determines the speed of the crumpling process, where a small value has been chosen to avoid rate dependence in the mechanical response and the final crumpled graphene structures. For the biaxial compression, the initially flat graphene sheet is placed in a three-dimensional rectangular box with an initial in-plane length L_0 and a fixed height H. During the compression process, the simulation box is compressed biaxially at the same strain rate of 10^8 s^{-1}. The thickness of the crumpled graphene is constrained by fixed height of the simulation box. Periodic boundary conditions are applied to the simulation box along the x and y (in-plane) directions. Non-terminated graphene (graphene) with dangling bonds and hydrogen-terminated graphene (H-graphene) are comparatively studied to examine edge effects on the crumpling process.

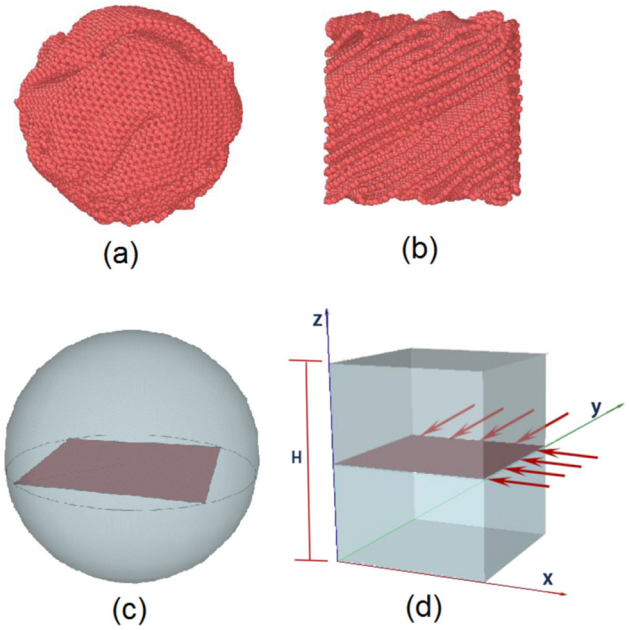

Figure 1. Structures for crumpled graphene of size 20 × 20 nm at room temperature obtained by (a) hydrostatic compression; (b) biaxial compression. (c) The illustration of hydrostatic compression where the graphene sheet is crumpled by shrinking a spherical shell. The analytical force $f(r) = k(r - R)^2$ is applied to each atom in the system, where k is the spring constant, r is the distance from the carbon atom to the center of the shell, and R is the shell radius. (d) The illustration of biaxial compression, where the graphene sheet is crumpled by shrinking the in-plane length of a three-dimensional rectangular box with a fixed height H.

MD simulations were performed using the large-scale atomic/molecular massively parallel simulator package [28]. The adaptive intermolecular reactive empirical bond order potential [29] was used to describe the interatomic interactions, which include both covalent and vdW interactions. The entire crumpling process was simulated within the NVT ensemble at 300 K. The standard Newton equations of motion were integrated in time using the velocity Verlet algorithm with a time step of 1 fs.

3. Results and discussions

3.1. Crumpled graphene from hydrostatic compression

We first investigate the crumpling process for graphene and H-graphene of dimension 20 × 20 nm by the hydrostatic compression. The degree of crumpling for hydrostatic compression can be measured by $1 - R/R_0$. Figure 2 displays some typical steps during the crumpling process.As can be seen from left to right in figure 2, the graphene sheet becomes increasingly compressed, where the degree of crumpling is represented by the increasing density of ridges and vertices [9]. First, the corners of the square graphene sheet will fold at the initial stage of the compression process. Then the central portion of the graphene bends gradually. Next, the self-adhesion

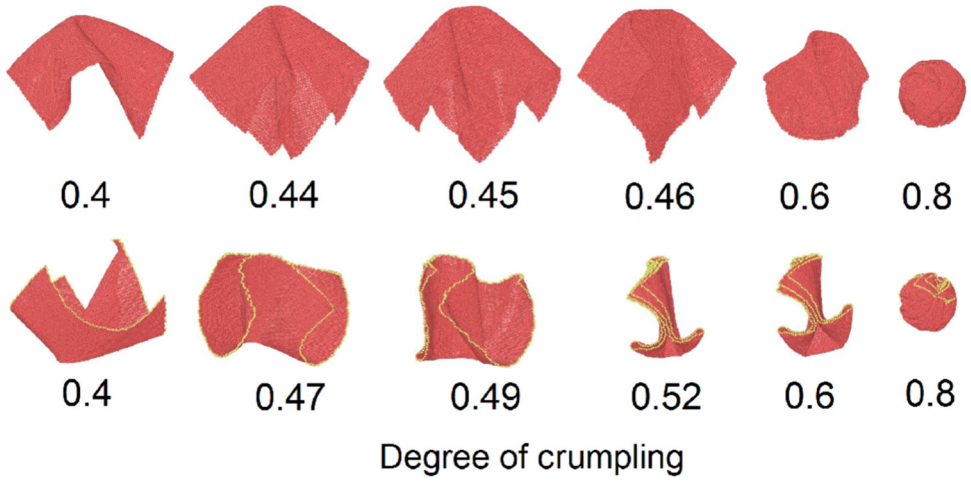

Figure 2. The snapshots of the crumpling process during the hydrostatic compression. The first and second lines represent graphene and H-graphene, respectively.

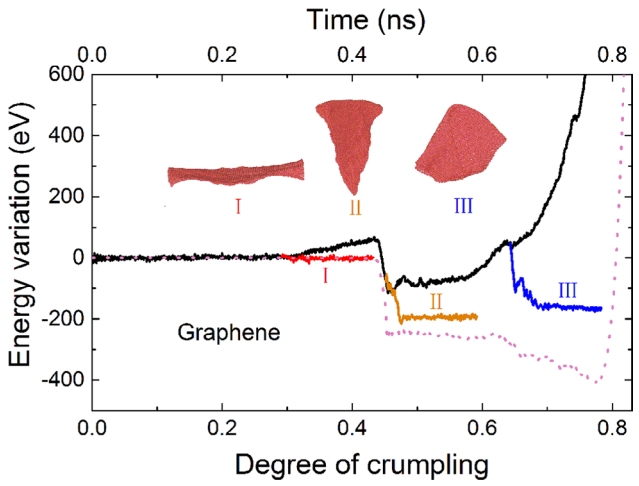

Figure 3. Potential energy variation (black line) during the hydrostatic crumpling of graphene. The magenta dotted line indicates the adhesion energy during the crumpling process. The inserts are the final configurations of the crumpled graphene at three different degrees of crumpling 0.30 (1), 0.45 (2) and 0.65 (3) after the external force is removed. The red, orange and blue lines correspond to the potential energy variation during the release process for the obtained crumpled graphene at degrees of crumpled graphene 0.30, 0.45 and 0.65, respectively. The decrease in adhesion energy is about −247 eV when the degree of crumpling is about 0.45 for the self-adhesion process.

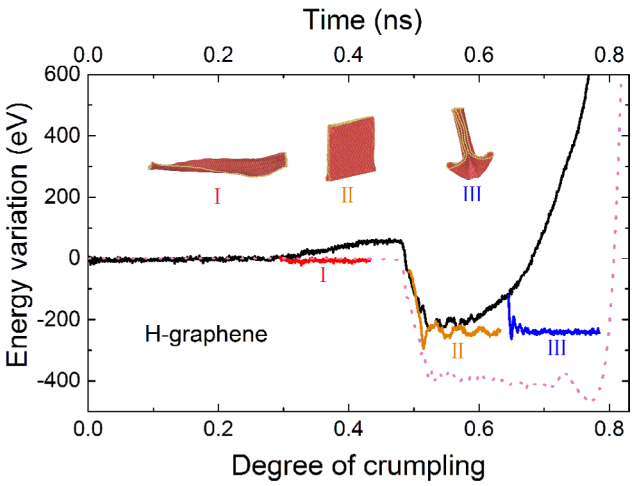

Figure 4. Potential energy variation (black line) during the hydrostatic crumpling processes of H-graphene. The magenta dotted line indicates the adhesion energy to the crumpling process. The inserts are the final configurations of the crumpled H-graphene at three different degrees of crumpling 0.30 (1), 0.49 (2) and 0.65 (3) after the external force is removed. The red, orange and blue lines correspond to the potential energy variation to simulation time during the release process for the obtained crumpled graphene at degrees of crumpled graphene 0.30, 0.49 and 0.65, respectively. The decrease in adhesion energy is about −383 eV when the degree of crumpling is about 0.5 for the self-adhesion process.

phenomenon happens, resulting in a rapid jump in the adhesion (or vdW) energy [5, 13, 26]. After the self-adhesion, new covalent bonds are formed that link the free edges together [22, 27, 30]. With further compression, various defects appear in graphene, including bond breaking and the formation of stone-wales defects. Finally, the crumpled graphene is compressed into a dense, spherical ball until compressive failure occurs.

More specifically, in figure 2, the two snapshots for the degree of crumpling 0.4 represent the bending of the central portion of graphene and H-graphene, respectively. In the first row in figure 2 for graphene, the snapshots at degrees of crumpling 0.44, 0.45 and 0.46 display the beginning, development and completion of the self-adhesion stage. The snapshot of graphene at degree of crumpling 0.6 reflects the formation of new covalent bonds and the linking together of free edges, which does not occur in H-graphene because of the hydrogenated-edges in H-graphene. Similarly, the snapshots of H-graphene at degrees of crumpling 0.47, 0.49 and 0.52 present the beginning, development and completion of the self-adhesion stage. However, H-graphene exhibits significantly more folding during the self-adhesion stage, which explains the larger drop in self-adhesion energy for H-graphene in figure 4 than graphene in figure 3.

During the crumpling of graphene or H-graphene, there is a competition between the adhesion energy and the bending energy [22, 27]. The adhesion energy has the tendency to adhere the surfaces of folds and crumples together

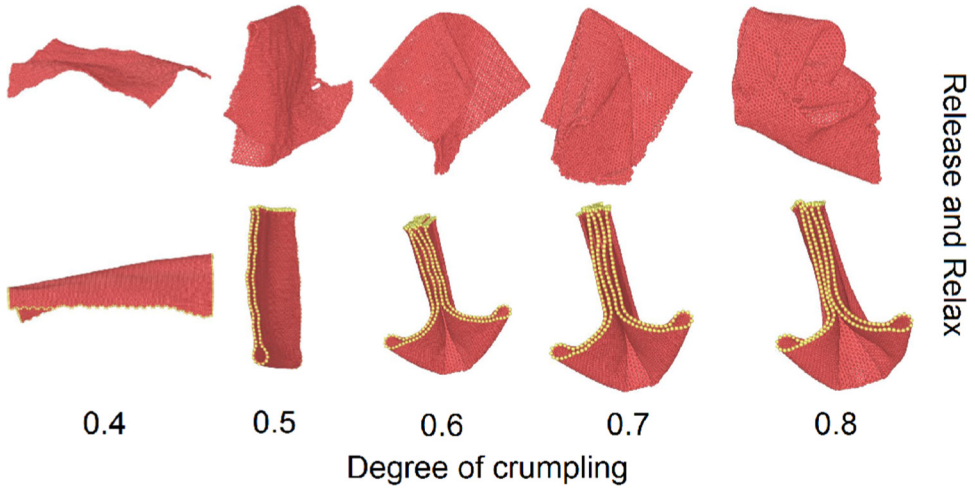

Figure 5. Snapshots of the final, relaxed structures obtained at different degrees of crumpling (0.4, 0.5, 0.6, 0.7 and 0.8) after removing the external hydrostatic force. The first and second lines represent graphene and H-graphene, respectively.

resulting in a more compact structure. On the other hand, the bending energy favors flattening out the crumpled graphene, and the stability and irreversibility of the crumpled graphene is determined by the competition between the adhesion energy and bending energy, as we will demonstrate analytically later in this paper. More specifically, the crumpled graphene will be stable if the crumpling induced decrease in the adhesion energy is larger than the increase of the bending energy.

We thus show in figures 3 and 4 the variation of potential energy during the crumpling process, which is similar to previous analyses for graphene [13]. For small degrees of crumpling, the initial folds do not cause any changes in the adhesion energy as the contact area is rather small. The self-adhesion phenomenon occurs at the degree of crumpling around 0.5 (0.45 for graphene or 0.49 for H-graphene respectively), where the adhesion and potential energies decline dramatically as shown in figures 3 and 4. As the degree of crumpling increases, the adhesion energy decreases gradually and reaches a minimum value for a degree of crumpling around 0.8.

We also examined the effect of releasing the hydrostatic external force for different degrees of crumpling to examine the irreversibility of the crumpling. As shown in the inset snapshots in figures 3 and 4, for some degrees of crumpling, the graphene and H-graphene sheets were able to return to a nearly flat configuration (I in figures 3 and 4) [27]. However, for other degrees of crumpling, the graphene sheets were unable to recover their initially flat configurations (II and III in figures 3 and 4), indicating the irreversible nature at those degrees of crumpling. Furthermore, previous results have shown that crumpled graphene cannot be transformed into a flat sheet through heating [26]. Figure 5 presents the fully relaxed structures of the crumpled graphene with different degrees of crumpling after the external force is removed; we will quantify later the factors governing whether the graphene sheets are crumpled reversibly or irreversibly.

3.2. Crumpled graphene from biaxial compression

We now show results of the simulation of crumpling graphene via biaxial compression subject to a fixed height constraint in the out-of-plane direction. For a given fixed height constraint H, the degree of crumpling is characterized by $\Delta L/L_0$, where L_0 is the initial length and ΔL is the compressed length. Figure 6 shows representative snapshots during the crumpling process of graphene with fixed height $H = 50.0$ and 90.0 Å. Some buckles and crumples appear gradually at the beginning of the compression. With the increase of strain, more random folds with ridges and vertices will emerge, similar to the observation in the experiment, [10] and then these folds are compressed together to form a compact structure. It can be seen that the fixed height H has an important effect on the configuration of crumpled graphene during the crumpling process. A higher fixed height will result in higher folds and less bending segments as shown in figure 6(b). In contrast, figure 6(a) shows that plenty of small random folds occur during the crumpling process for a lower fixed height 50 Å.

The irreversibility of the crumpled graphene is determined by the competition between adhesion energy and bending energy. Figure 7 shows the variation of adhesion energy during the crumpling process. For a given fixed height H, the adhesion energy decreases gradually with the increase of degree of crumpling, as the effective contact area increases. There is a step-like jump in the adhesion energy at a critical degree of crumpling, where the self-adhesion happens. For a low fixed height H ($30 \leqslant H \leqslant 50$) as shown in figure 7(a), the self-adhesion phenomenon is relatively weak, because of the height constraint. Figure 8 illustrates that the crumpled graphene becomes irreversible if the degree of crumpling is larger than the critical value 0.61 for $H = 40$ Å. Specifically, the crumpled graphene is able to regain its initially flat state if the biaxial compression is removed for the degree of crumpling of 0.55, while the crumpled graphene cannot fully recover its planar configuration for degrees of crumpling above 0.61.

For a high fixed height H ($H \geqslant 60$) as shown in figure 7(b), the self-adhesion phenomenon is clearly evident. The crumpled

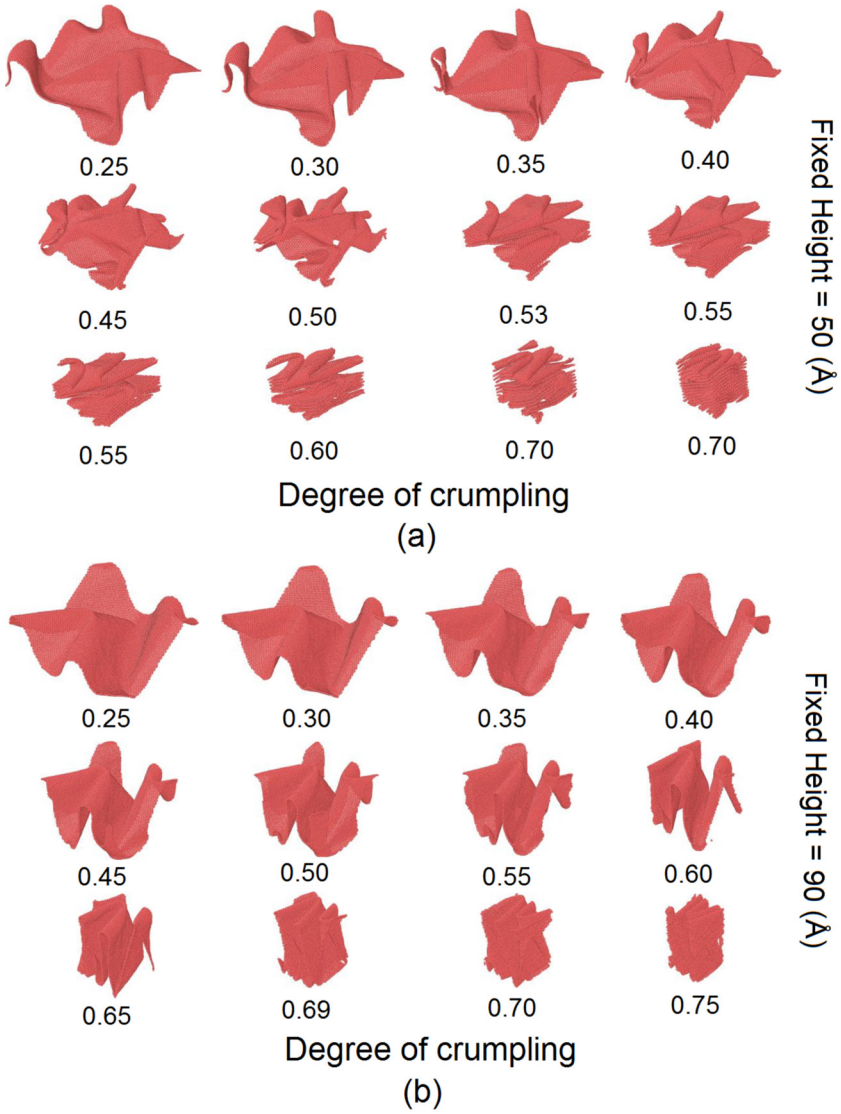

Figure 6. Snapshots of the crumpling process during the biaxial compression of graphene with a height constraint of (a) 50 Å; (b) 90 Å.

graphene will be stable if the crumpling induced jump (or decrease) for the adhesion energy is larger than the increase of the bending energy. Figure 9 illustrates that the critical degree to obtain an irreversible crumpled graphene is 0.55 for $H = 90$ Å. For example, graphene can regain its initially flat state for degree of crumpling of 0.43, while the crumpled graphene becomes irreversible for the degrees of crumpling above 0.55.

Figure 10 (lower curve) summarizes the critical degree of crumpling corresponding to different fixed height with the size 20×20 nm. The critical degrees of crumpling fluctuate around 0.55. The crumpled graphene can recover its planar configuration in region A, while the crumpling process is irreversible in region B. The upper, red curve corresponds to the maximum value of the degree of crumpling, above which the crumpled graphene undergoes compressive failure. To illustrate the size-dependence of the crumpling, we show in figure 11 the result of a smaller, 10×10 nm graphene sheet. The available phase space for irreversible crumpling similar to the B region in figure 10 is greatly reduced, as the crumpling process becomes irreversible only when the degree of crumpling is close to the compressive failure. We note that when the length of the graphene sheet in one direction exceeds the minimum length of 14.6 nm, which we will explain later, the self-adhered graphene becomes stable. Clearly, the graphene sheet must have a minimum length in order to for the crumpling to be irreversible.

3.3. Analytic model for the reversibility of crumpled graphene

The above figures 3, 4 and 7 show that the crumpling process becomes irreversible after a step-like jump in the adhesion energy at a critical degree of crumpling. In other words, the crumpling process becomes irreversible if the adhesion energy is reduced enough. We will discuss a critical value for the adhesion energy corresponding to the critical degree of crumpling.

Figure 12 shows the stable structure of a single fold in graphene with different boundary conditions. Figure 12(a) displays a graphene fold with periodic boundary condition

in the horizontal direction. Figure 12(b) shows a single fold with free edges. Figure 12(c) shows a graphene fold with H-terminated edges.

The total energy of the folding graphene with respective to its planar configuration can be obtained analytically [31]. The definition of geometrical parameters can be found in figure 12. The total energy for the graphene fold in figure 12(a) is given by

$$E_1 = \frac{D}{2}\left(\frac{\pi}{R_b} + 2\frac{\theta_1}{R_1} + 2\frac{\theta_2}{R_2}\right)W - \beta\lambda W, \tag{1}$$

where $D = 1.2931$ eV is the bending stiffness per width length, $\beta = 0.02$ eV Å^{-1} is the adhesion energy density [31] and W is the width of the graphene sheet. The geometrical parameters θ_1, θ_2, R_1, R_2, and R_b are listed in table 1, which are obtained from the relaxed configuration from MD simulations. The first term in equation (1) is the bending energy, and the second term in equation (1) is the adhesion energy. The total energy can be expressed in terms of the total length,

$$E_1 = 0.6922DW - \frac{\beta}{2}(L - 56.6132)W. \tag{2}$$

Similarly, the total energy for graphene folds shown in figures 12(b) and (c) is given by

$$E_2 = \frac{D}{2}\left(2\frac{\theta_1}{R_1} + 2\frac{\theta_2}{R_2}\right)W - \beta\lambda W. \tag{3}$$

It can be expressed in terms of the total length,

$$E_2 = 0.4934DW - \frac{\beta}{2}(L - 31.8132)W. \tag{4}$$

For obtaining the stable folded structures as shown in figure 12, the total length L should be large enough to make sure the total system energy is less than zero. We obtain the minimum values from the analytic model, by constraining the total system energy in equations (2) and (4) to be zero. Accordingly, we find that the minimum values of the total length are 14.6 nm and 9.6 nm for the biaxial and hydrostatic compression, respectively.

For the hydrostatic compression, a stable irreversible fold as shown in figures 12(b) or (c) can be obtained as long as the decrease in self-adhesion energy is equal to the bending energy of the fold. That is the critical adhesion energy E_{ca} for graphene or H-graphene can be calculated following the first term in equation (4). In particular, for H-graphene, $E_{ca} = -0.4934DW = -0.4934 * 1.2931 * 200$ eV $= -128$ eV. As the self-adhered fold for graphene is formed diagonally as shown in figure 3, the critical adhesion energy for graphene is calculated as $E_{ca} = -0.4934DW = -179$ eV. We find that this critical adhesion energy can be used as a criterion for the irreversibility of the crumpled graphene from hydrostatic compression shown in figure 3. If the decrease of the adhesion energy induced by the self-adhesion is larger than E_{ca}, then the resultant crumpled graphene is irreversible after the external constraints are removed. Otherwise, the crumpled graphene is reversible if the change of the adhesion energy is less than E_{ca} during the self-adhesion phenomenon.

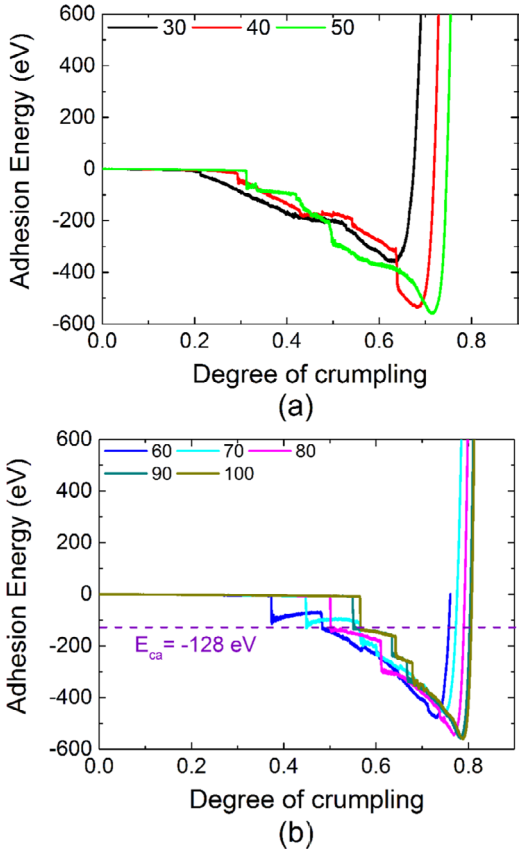

Figure 7. The adhesion energy during the crumpling process (a) for small fixed heights H, i.e. $30 \leqslant H \leqslant 50$; (b) for larger fixed heights H, i.e. $H \geqslant 60$. $E_{ca} = -128$ eV is the critical value of the adhesion energy for the high fixed height constraint for irreversible crumpling to occur.

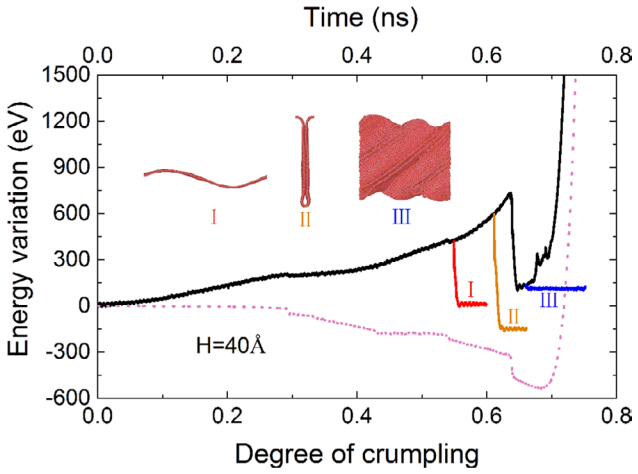

Figure 8. The energy variation to the crumpling processes of the crumpled graphene with fixed height 40 Å. The black line indicates the potential energy variation to the crumpling process. The magenta dot line indicates the adhesion energy to the crumpling process. The inserts are the final configurations of the obtained crumpled graphene at three different degrees of crumpling 0.55 (1), 0.61 (2) and 0.66 (3) during the release process. The red, orange and blue lines correspond to the potential energy variation to simulation time during the release process for the obtained crumpled graphene at degrees of crumpled graphene 0.55, 0.61 and 0.66, respectively.

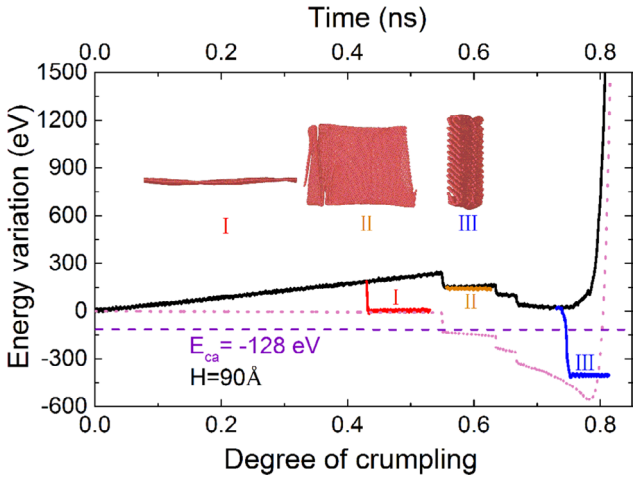

Figure 9. The energy variation to the crumpling processes of the crumpled graphene with fixed height 90 Å. The black line indicates the potential energy variation to the crumpling process. The magenta dot line indicates the adhesion energy to the crumpling process. The inserts are the final configurations of the obtained crumpled graphene at three different degrees of crumpling 0.43 (1), 0.55 (2) and 0.73 (3) during the release process. The red, orange and blue lines correspond to the potential energy variation to simulation time during the release process for the obtained crumpled graphene at degrees of crumpled graphene 0.43, 0.55 and 0.73, respectively.

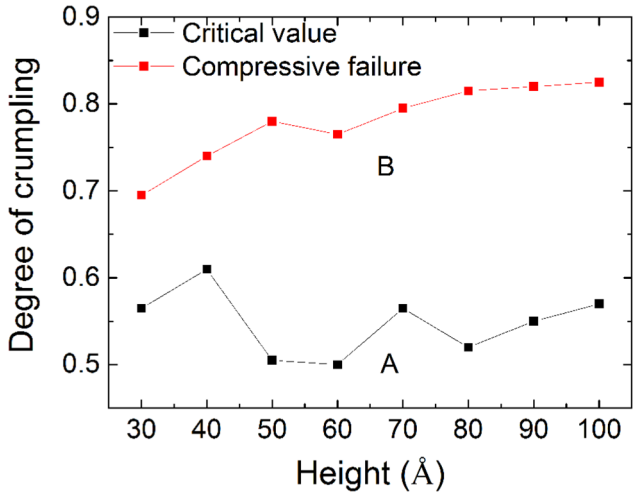

Figure 10. The steady state of crumpled graphene sheets with the size 20 × 20 nm obtained by the biaxial compression. The crumpled graphene sheets in the A region will lose stability during relaxation and develop into flat sheets. In contrast, the crumpled graphene sheets in the B region cannot be flattened during relaxation. The black line for the critical degree of crumpling fluctuates around 0.55.

For the biaxial compression with a low fixed height H ($30 \leqslant H \leqslant 50$), the decrease in self-adhesion energy is too small to form an irreversible self-adhered crumpled graphene as shown in figure 7. As a result, the critical degree of crumpling for the irreversible crumpled graphene is difficult to be determined by the adhesion energy. The simulation results for the low height in figure 10 show that the critical degrees of crumpling is around 0.55. For the biaxial compression with a high fixed height H ($H \geqslant 60$), there is a remarkable self-adhesion. The top bending part in the fold has the tendency

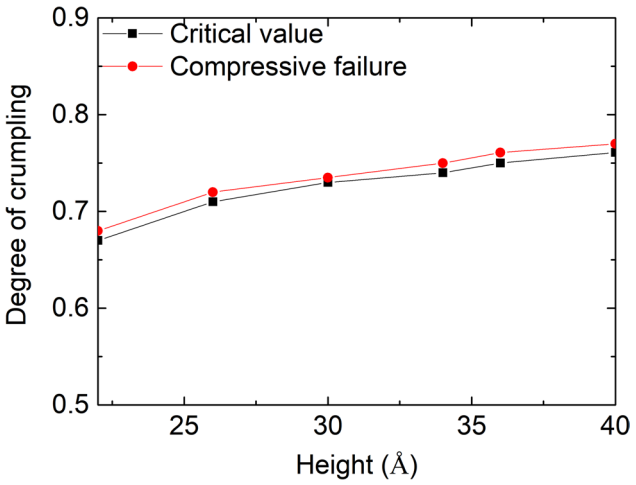

Figure 11. The steady state of crumpled graphene sheets with the size 10 × 10 nm obtained by biaxial compression. Compared with the result of graphene with the size 20 × 20 nm, the available area for the irreversible crumpling similar to the B region in figure 10 is greatly reduced.

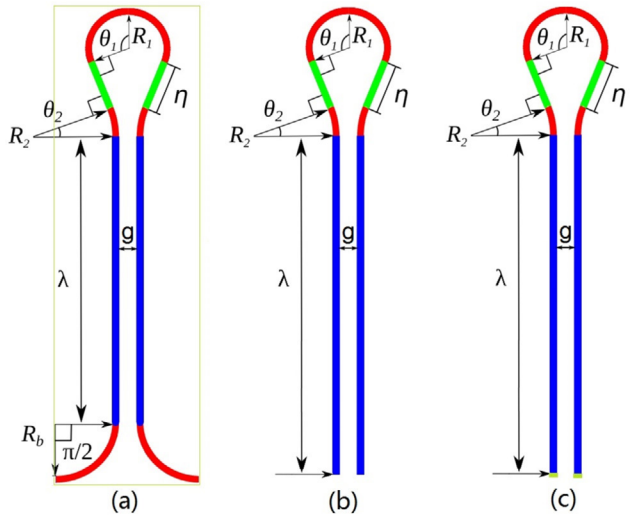

Figure 12. The different crumpled graphene folds. (a) A stable fold with periodic boundary. (b) A stable fold with free boundary. (c) A stable fold with free boundary and hydrogen-terminated edge.

Table 1. Geometrical parameters (in Å) for the crumpled graphene fold.

Parameters	η	R_1	R_2	R_b	θ_1	θ_2
Value	6.4476	3.8685	9.9937	7.8983	1.8142	0.2442

to flatten the fold, so the crumpled graphene will be irreversible as long as the decrease in self-adhesion energy is equal to or larger than the bending energy of the top part of fold as shown in figure 12(a). As a result, the critical adhesion energy can be calculated by the first term of equation (4); i.e. $E_{ca} = -0.4934DW = -128$ eV. This critical adhesion energy can be used as a criterion for the irreversibility of the crumpled graphene shown in figure 9. The result also shows that the critical degrees of crumpling are around 0.55.

We point out that, the critical degrees of crumpling are around 0.5 or 0.55 for hydrostatic and biaxial compression,

respectively. These values are geometrically related to the folded configuration shown in figure 12. When a piece of graphene sheet is folded into the stable folding structure, it can be considered as a crumpled sheet of graphene with a degree of crumpling of 0.5, which explains the critical value for the degree of crumpling from MD simulations. The stable folded structure as obtained from the analytic model thus sufficiently accounts for the importance of adhesion energy, and is consistent with the dynamic crumpling process observed in the MD simulations. Importantly, the analytic model predicts that to obtain irreversibly crumpled graphene, the degree of crumpling should be at least 0.5, which demonstrates good agreement between the MD simulations and the analytic model.

4. Conclusion

In summary, using classical molecular dynamics we have investigated the mechanics of how graphene crumples subject to hydrostatic or biaxial compression. We find that in both cases, graphene exhibits a critical degree of crumpling of about 0.5 or 0.55 for hydrostatic and biaxial compression, respectively, above which graphene is irreversibly crumpled after the removal of external constraints. The critical degree of crumpling is closely related to the self-adhesion phenomenon of graphene, which leads to a step-like decrease in the adhesion energy. The MD simulation results match analytic solutions balancing bending and adhesive energies to determine the critical degree of crumpling. Compared with flat graphene, crumpled graphene has shown many unique properties [9, 14], which will attract much interest. Considering that most of the current studies on crumpled graphene are based on graphene with small aspect ratio, and because the aspect ratio usually affects the mechanical response of graphene, it will be important to study the aspect ratio effect on the crumpling process in the future.

Acknowledgments

The work is supported by the Recruitment Program of Global Youth Experts of China, the National Natural Science Foundation of China (NSFC) under Grant No. 11504225 and the start-up funding from Shanghai University. HSP acknowledges the support of the Mechanical Engineering department at Boston University.

ORCID iDs

Jing Wan https://orcid.org/0000-0002-7261-1957
Jin-Wu Jiang https://orcid.org/0000-0002-8287-5606

References

[1] Vandeparre H, Pineirua M, Brau F, Roman B, Bico J, Gay C, Bao W, Lau C N, Reis P M and Damman P 2011 *Phys. Rev. Lett.* **106** 224301
[2] Bouaziz O, Masse J, Allain S, Orgéas L and Latil P 2013 *Mater. Sci. Eng.* A **570** 1
[3] Deboeuf S, Katzav E, Boudaoud A, Bonn D and Adda-Bedia M 2013 *Phys. Rev. Lett.* **110** 104301
[4] Lindahl N, Midtvedt D, Svensson J, Nerushev O A, Lindvall N, Isacsson A and Campbell E E 2012 *Nano Lett.* **12** 3526
[5] Fasolino A, Los J H and Katsnelson M I 2007 *Nat. Mater.* **6** 858
[6] Bao W, Miao F, Chen Z, Zhang H, Jang W, Dames C and Lau C N 2009 *Nat. Nanotechnol.* **4** 562
[7] Kim K, Lee Z, Malone B D, Chan K T, Alemán B, Regan W, Gannett W, Crommie M, Cohen M L and Zettl A 2011 *Phys. Rev.* B **83** 245433
[8] Ramanathan T *et al* 2008 *Nat. Nanotechnol.* **3** 327
[9] Luo J, Jang H D, Sun T, Xiao L, He Z, Katsoulidis A P, Kanatzidis M G, Gibson J M and Huang J 2011 *Acs Nano* **5** 8943
[10] Zang J, Ryu S, Pugno N, Wang Q, Tu Q, Buehler M J and Zhao X 2013 *Nat. Mater.* **12** 321
[11] Liu C, Yu Z, Neff D, Zhamu A and Jang B Z 2010 *Nano Lett.* **8** 4863
[12] Stoller M D, Park S, Zhu Y, An J and Ruoff R S 2008 *Nano Lett.* **8** 3498
[13] Cranford S W and Buehler M J 2011 *Phys. Rev.* B **84** 205451
[14] Pereira V M, Neto A C, Liang H and Mahadevan L 2010 *Phys. Rev. Lett.* **105** 156603
[15] Jin Z, Lu W, ONeill K J, Parilla P A, Simpson L J, Kittrell C and Tour J M 2011 *Chem. Mater.* **23** 923
[16] Chen Y *et al* 2012 *Nano Lett.* **12** 1996
[17] Liu F, Song S, Xue D and Zhang H 2012 *Adv. Mater.* **24** 1089
[18] Lee W-K, Kang J, Chen K-S, Engel C J, Jung W-B, Rhee D, Hersam M C and Odom T W 2016 *Nano Lett.* **16** 7121
[19] Levy N, Burke S A, Meaker K L, Panlasiguri M, Zettl A, Guinea F, Neto A H C and Crommie M F 2010 *Science* **329** 544
[20] Guinea F, Katsnelson M I and Geim A K 2010 *Nat. Phys.* **6** 30
[21] Baimova J A, Dmitriev S V, Zhou K and Savin A V 2012 *Phys. Rev.* B **86** 035427
[22] Baimova J A, Liu B, Dmitriev S V and Zhou K 2015 *J. Phys. D: Appl. Phys.* **48** 095302
[23] Compton O C, Kim S, Pierre C, Torkelson J M and Nguyen S T 2010 *Adv. Mater.* **22** 4759
[24] Zhu Y *et al* 2011 *Science* **332** 1537
[25] Han X *et al* 2017 *ACS nano* **11** 3189
[26] Tallinen T, Åström J, Kekäläinen P and Timonen J 2010 *Phys. Rev. Lett.* **105** 026103
[27] Chang C, Song Z, Lin J and Xu Z 2013 *RSC Adv.* **3** 2720
[28] Plimpton S J 1995 *J. Comput. Phys.* **117** 1
[29] Stuart S J, Tutein A B and Harrison J A 2000 *J. Chem. Phys.* **112** 6472
[30] Cai K, Wan J, Yu J, Cai H and Qin Q 2016 *Appl. Surf. Sci.* **377** 213
[31] Zhang Y, Wei N, Zhao J, Gong Y and Rabczuk T 2013 *J. Appl. Phys.* **114** 063511